Coupled Cluster Green's Functions for Periodic Systems: Ab-initio computation and applications

Thesis by
Jason M. Yu

In Partial Fulfillment of the Requirements for the
Degree of
Master of Science

CALIFORNIA INSTITUTE OF TECHNOLOGY
Pasadena, California

2019
Defended June 14, 2019

Jason M. Yu
ORCID: 0000-0002-2270-6798

ACKNOWLEDGEMENTS

I would like to thank Narbe Mardirossian, James McClain, and Qiming Sun for their guidance during my graduate studies. I also thank Garnet Chan and the Chan group for their advice and knowledge. Support from the National Science Foundation Graduate Research Fellowship Program is acknolwedged.

ABSTRACT

The Coupled Cluster Green's function method is expanded to periodic systems and preliminary results of the spectral function for diamond and graphene are shown. Future improvements and potential applications are discussed.

TABLE OF CONTENTS

LIST OF ILLUSTRATIONS

Chapter 1

INTRODUCTION

Single-particle Green's function-based methods have become popular tools in the field of condensed matter physics and materials science to describe the electronic structure of solid systems [1]. Knowledge of the Green's function, which is a propagator that describes the movement of an electron in a many-body potential, gives access to important properties including excited states, transition moments, and response functions. Such properties are imperative to the study of technologically important materials, like those with light-harvesting or superconducting characteristics.

The Green's function is typically found through solving the Dyson equation, where it incorporates the renormalization of single-particle states due to many-body interactions by introducing the concept of self-energy. This quantity can be represented as a series of perturbation diagrams, and used to evaluate the Dyson equation diagramatically. The most commonly used technique to estimate the self-energy involves expanding it to first order in terms of a screened interaction W, and is known as the *G.W.* approximation [2, 3].

The *G.W.* approximation has been successful in describing the electronic structure of many crystalline systems [4]. However, because this method is only a first approximation to the self-energy, which is a complicated function describing the many-body interaction, it fails when considering problems with strong correlation or when greater accuracy is needed. For example, it continues to overestimate total energies and band gaps, and is often unable to detect satellite structures [5]. Modifications to the theory, such as inclusion of vertex corrections, improve its performance somewhat, but many issues still persist [6]. These observations illustrate the difficulty associated with systematically improving *G.W.* theory through inclusion of higher-order self-energy terms. Better approximations to the single-particle Green's Function of many-body systems are thus needed to improve the accuracy of electronic structure predictions for solids.

Coupled Cluster (CC) theory has been considered in the past as an avenue towards this goal. The concept behind a CC approach to approximating the single-particle Green's function (CCGF) was first introduced by Nooijen and Bartlett [7, 8], and the

method was recently implemented by Bhaskaran et al. to estimate the self-energy associated with molecular systems [9]. Several advantages over the more traditional approaches to the Green's function are apparent in the Coupled Cluster framework: the Dyson equation does not need to be solved unlike in $G.W.$ theory, the exact many-body wavefunction limit exists through including higher excitations (S, D, T, etc), and it shares a similar foundation with the EOM Coupled Cluster (EOM-CC) approach to excited states. Here, we outline a CCGF approach in the spirit of these two predecessors expanded to periodic systems, which we now abbreviate as (KCCGF). The leading "K" has been chosen to allude to the momentum-space wavevector k.

First, a brief introduction to quantum Green's functions will be given along with their use as propagators to investigate electronic properties. Next, the guiding equations of Periodic Coupled Cluster theory will be reviewed as it is implemented in the quantum chemistry code PySCF [10]. Finally, the KCCGF method will be described along with its computational details and a proof-of-concept calculation for the band structure of Diamond. We will conclude with further areas for improvement of the cost and accuracy of the KCCGF method.

Chapter 2

QUANTUM GREEN'S FUNCTIONS

Before describing the KCCGF method, the basic properties of Green's functions will be outlined. This brief review is based on the pedagogical text by Odashima [11], which can be used as an additional reference if necessary.

We first introduce the single-particle electron Green's Function through Feynman's quantum field propagator:

$$G^c_{ij}(t,t') = -i < T[c_i(t), c^\dagger_j(t')] > \tag{2.1}$$

Which contains a time-ordering operator T that guarantees causality with respect to time. Note that the superscript c denotes this term as the "causal" Green's function. To illustrate, $c^\dagger_j$ creates an electron at the jth site at $t' < t$ and c_i annihilates it at the ith site at time t. A hole is conversely created at the ith site at time $t < t'$, and annihilated at the jth site at time t'. The time-ordering operator serves to prevent instances where an electron or hole is annihilated before it is created. Here, the creation and annihilation operators are expressed in a discrete particle basis.

This behavior can also be illustrated by the action of the time-ordering operator,

$$T[c_i(t)c^\dagger_j(t')] = \theta(t-t')c_i(t)c^\dagger_j(t') - \theta(t'-t)c^\dagger_j(t')c_i(t) \tag{2.2}$$

Knowing the general structure, it is now time to introduce two flavors of Green's functions which have the benefit of being easily analyzed to extract physical quantities. These are known as the retarded and advanced Green's functions:

$$G^r_{ij}(t,t') = -i\theta(t-t') < \{c_i(t), c^\dagger_j(t')\} > \tag{2.3}$$

$$G^a_{ij}(t,t') = i\theta(t'-t) < \{c^\dagger_i(t), c_j(t')\} > \tag{2.4}$$

The retarded Green's function is non-zero only for times $t < t'$, such that the response of the system can be calculated after it has been perturbed. The advanced Green's function is the adjoint of the retarded Green's function.

The benefits of writing the Green's function in the retarded and advanced forms can be shown for the non-interacting case and then generalized to an interacting

many-body system. If we consider the second quantized free-particle Hamiltonian, we find:

$$H = \sum_n \epsilon_n c_n^\dagger c_n \tag{2.5}$$

In the Heisenberg picture, we can work out that the equations of motion for the creation/annihilation operators are

$$\frac{dc_n}{dt} = -i[c_n, H] = -i\epsilon_n c_n \tag{2.6}$$

$$\frac{dc_n^\dagger}{dt} = -i[c_n^\dagger, H] = i\epsilon_n c_n^\dagger \tag{2.7}$$

Solving this differential equation, we find how these operators evolve with time.

$$c_n(t) = e^{-i\epsilon_n t} c_n \tag{2.8}$$

$$c_n^\dagger(t) = e^{i\epsilon_n t} c_n^\dagger \tag{2.9}$$

With this, we can substitute into the expressions for the retarded and advanced Green's functions and evaluate the contents of the expectation value. Thus, for this free particle Hamiltonian, we find the Green's functions as:

$$G^r_{nn'}(t-t') = -i\theta(t-t')e^{-i\epsilon_n(t-t')}\delta_{nn'} \tag{2.10}$$

$$G^a_{nn'}(t-t') = i\theta(t'-t)e^{i\epsilon_n(t'-t)}\delta_{nn'} \tag{2.11}$$

We consider the analytical expression for the step function:

$$\theta(t-t') = -\frac{1}{2\pi i}\int_{-\infty}^{\infty} d\omega \frac{e^{-i\omega(t-t')}}{\omega + i\eta}, \tag{2.12}$$

and substitute this into our expression for the retarded Green's function (we limit to just this variant for the rest of this secton).

$$G^r_{nn}(t-t') = \frac{1}{2\pi}\int_{-\infty}^{\infty} d\omega \frac{e^{-i\omega(t-t')}}{\omega - \epsilon_n + i\eta} \tag{2.13}$$

Where we made a change of variables

$$\omega + \epsilon_n \equiv \omega \tag{2.14}$$

If we define the Fourier transform and its inverse as

$$G^r_{ij}(t-t') = \frac{1}{2\pi}\int_{-\infty}^{\infty} d\omega\ e^{-i\omega(t-t')} G^r_{ij}(\omega) \tag{2.15}$$

$$G^r_{ij}(\omega) = \int_{-\infty}^{\infty} dt\ e^{i\omega t} G^r_{ij}(t), \tag{2.16}$$

we immediately see that the retarded Green's function in Fourier representation is

$$G^r_{nn}(\omega) = \frac{1}{\omega - \epsilon_n - i\eta}, \tag{2.17}$$

and can be written in an orbital basis with a resolution of the identity:

$$G^r_{ij}(\omega) = \sum_n \frac{< i|n >< n|j >}{\omega - \epsilon_n + i\eta} \tag{2.18}$$

This form of the retarded Green's function demonstrates its convenience in obtaining eigenergies ϵ_n, as they occur with the poles of the function.

This structure can be generalized to an interacting system, and the corresponding interacting Green's Function can be expressed in the Lehmann representation at zero temperature.

$$G^r_{ij}(\omega) = \sum_{nm} \frac{< n|c_i|m >< m|c^\dagger_j|n >}{\omega - (\epsilon_n - \epsilon_m) + i\eta} + \frac{< m|c_i|n >< n|c^\dagger_j|m >}{\omega - (\epsilon_m - \epsilon_n) + i\eta} \tag{2.19}$$

The differences in eigenenergies, $-(\epsilon_n - \epsilon_m)$ that arise in this case will be useful when using our KCCGF method to calculate quasiparticle energies, which are known as the difference in energy between the ground state and $N + 1$ or $N - 1$ electron excited states.

Chapter 3

COUPLED CLUSTER THEORY

Coupled Cluster theory has gained a reputation as one of the most successful wavefunction based quantum chemistry techniques affordable with modern computational resources. This is in large part due to its ability to accurately predict ground and excited state properties while maintaining size consistency and a hierarchial structure [12, 13]. Building upon a reference determinant obtained from mean-field methods, Coupled Cluster explicitly incorporates correlation due to many-body electronic interactions, which plays a key role in most physical systems. Although the method has a significant computational cost, it offers a clear avenue towards approximating the exact many-body wavefunction, coming into its own as a desirable compromise between mean-field and expensive Configuration Interaction methods.

With the numerous benefits of the Coupled Cluster approximation, it is natural to consider how the method can be applied to periodic systems. Recently, the Chan group has made this possible through their work expanding Coupled Cluster theory to solids for both the ground and excited states [14]. Here, we give a brief overview of Periodic Coupled Cluster as a precursor to our discussion of the KCCGF method. We start with a general picture before getting into specific practices for periodic systems.

The basic tenant of Coupled Cluster theory lies in its introduction of a cluster function which correlates the motion of electrons. The following expression corresponds to a two-particle cluster function.

$$f_{ij}(x_m, x_n) = \sum_{a>b} t_{ij}^{ab} \phi_a(x_m)\phi_b(x_n) \tag{3.1}$$

The cluster coefficients t are determined in the solution to the Schrodinger equation and ϕ represents general single-particle functions. By inserting this particular function into a general reference determinant, one obtains an improved wavefunction which accounts for the correlation of any pair of electrons within the specified occupied orbitals i and j. Note that we limit the following example to a four electron system represented by the determinant $\Phi_0 = |\phi_i(x_1)\phi_j(x_2)\phi_k(x_3)\phi_l(x_4) >$

to illustrate.

$$\begin{aligned}\Psi &= \Phi_0 + \sum_{a>b} t_{ij}^{ab} |\phi_a(x_1)\phi_b(x_2)\phi_k(x_3)\phi_l(x_4) > \\ &= |\Phi_0 + f_{ij}(x_m, x_n)\phi_k(x_3)\phi_l(x_4) >\end{aligned} \tag{3.2}$$

The inclusion of the cluster operator in the wavefunction is reflected in the additional determinant seen above with occupied orbitals i and j replaced with virtual orbitals a and b.

One can imagine that including additional cluster functions for different numbers of electrons will further serve this effect, and if every possible grouping of N electrons were included we would obtain the exact wavefunction for the basis. In second quantization, we may define general cluster operators as such:

$$\hat{T}_n = \left(\frac{1}{n!}\right)^2 \sum_{ij..ab..}^{n} t_{ij..}^{ab..} c_a^\dagger c_b^\dagger .. c_j c_i \tag{3.3}$$

It can be shown that if we write out the wavefunction of a system that includes all cluster operators of n orbitals, the resulting expression resembles a power series that may be succintly represented by an exponential function. We may thus write a general form of this Coupled Cluster wavefunction in the "exponential ansatz" known as :

$$\Psi = e^{\hat{T}} |\Phi_0 > \tag{3.4}$$

The coefficients of the $\hat{T}$ operator determine the properties of the Coupled Cluster wavefunction, and thus need to be found if we wish to use it in our subsequent computation of Green's Functions. The most common truncation of the $\hat{T}$ operator comes at the Singles and Doubles level, or $\hat{T} = \hat{T}_1 + \hat{T}_2$. At this level, the coefficients may be determined from the following two equations:

$$0 =< \Phi_i^a | \bar{H} | \Phi_0 > \tag{3.5}$$

and

$$0 =< \Phi_{ij}^{ab} | \bar{H} | \Phi_0 > \tag{3.6}$$

which are called the CCSD amplitude equations. These can be derived from the left projection of singly and doubly excited reference determinants onto the time-independent electronic Schrodinger equation $e^{-\hat{T}} \hat{H} e^{\hat{T}} |\Phi_0 >= E|\Phi_0 >$, taking into account that $\bar{H} = e^{-\hat{T}} \hat{H} e^{\hat{T}}$. Note that the above two equations arise from the fact that singly and doubly excited determinants are orthogonal to that of the ground state.

These equations can be solved iteratively, using either Wick's theorem or a diagrammatic method to evaluate the allowed contractions between the Hamiltonian and

cluster operators. Derivations of the explicit amplitude equations for CCSD and higher levels can be found in the literature [15, 16].

So far, the Coupled Cluster method as described has been for general many-body systems represented by the Hamiltonian $\hat{H}$. In our consideration of periodic systems, we take into account the dependence of the various operators on the momentum-space wavevector k. This is done because the operators of crystalline systems possess translation invariance and the orbitals obey Bloch's theorem, which enforces that the crystal momentum be conserved if we assume that there are no defects:

$$\sum_{a} k_a - \sum_{i} k_i = G, \tag{3.7}$$

where G is a lattice vector in reciprocal space and k_a and k_i are the relevant virtual and occupied orbital momenta. We rewrite $\hat{T}$ as:

$$\hat{T}_n = \left(\frac{1}{n!}\right)^2 {\sum_{k_i k_j .. k_a k_b ..}}' \sum_{ij..ab..}^{n} t_{ik_i jk_j ..}^{ak_a bk_b ..} c_{ak_a}^{\dagger} c_{bk_b}^{\dagger} .. c_{jk_j} c_{ik_i}, \tag{3.8}$$

with the primed sum indicating the conservation of momentum. The amplitude equations can now be revised, yielding:

$$0 = < \Phi_{ik_i}^{ak_a} | \bar{H} | \Phi_0 > \tag{3.9}$$

and

$$0 = < \Phi_{ik_i jk_j}^{ak_a bk_b} | \bar{H} | \Phi_0 > \tag{3.10}$$

Working equations for the above may be found in the literature [17]. For additional details regarding the implementation of Periodic Coupled Cluster, including integral generation and construction of the mean-field, see reference [14]. After solving these equations for the k-dependent T amplitudes, we acquire the Coupled Cluster description of the many-body wavefunction, a pre-requisite for KCCGF.

Chapter 4

PERIODIC COUPLED CLUSTER GREEN'S FUNCTIONS

As stated in previous sections, the guiding idea of KCCGF is to use the Coupled Cluster approximation of the many-body wavefunction to compute a Green's function that yields high accuracy observables for periodic systems. We now describe the theory behind Periodic Coupled Cluster Green's Functions, going beyond Nooijen and Bartlett's initial theory for molecules [8].

The non-hermiticity of our similarity transformed Hamiltonian, $\bar{H}$, indicates that our right and left ground state determinants are not simple adjoints of one another. We thus use the "bi-variational" ansatz to represent them:

$$< \Psi_0| \; = < \Phi|(1 + \Lambda)e^{-\hat{T}} \tag{4.1}$$

$$|\Psi_0 > = \; e^{\hat{T}}|\Phi >, \tag{4.2}$$

where the k-dependence of the operators $\hat{T}$ and Λ are implicit and we define Λ, a de-excitation operator, simply as

$$\Lambda \; = \; \sum_{n=1}^{N} \Lambda_n \; = \; \sum_{k_i k_j .. k_a k_b ..} \sum_{ij..ab..}^{n} \lambda_{ik_i jk_j ..}^{ak_a bk_b ..} c_{ak_a}^{\dagger} c_{bk_b}^{\dagger} .. c_{jk_j} c_{ik_i} \tag{4.3}$$

In this ansatz, we write the expression for the Green's function as:

$$G_{pk_p,qk_q}(\omega) = < \Phi|(1 + \Lambda)\bar{c}_{qk_q}^{\dagger}(\omega + (\bar{H} - E_0) - i\eta)^{-1}\bar{c}_{pk_p}|\Phi > \tag{4.4}$$

$$+ < \Phi|(1 + \Lambda)\bar{c}_{pk_p}(\omega - (\bar{H} - E_0) + i\eta)^{-1}\bar{c}_{qk_q}^{\dagger}|\Phi > \tag{4.5}$$

Where we have absorbed the factors of $e^{\hat{T}}$ into our operators, for instance:

$$\bar{c}_{pk_p} = e^{-\hat{T}} c_{pk_p} e^{\hat{T}} \tag{4.6}$$

The form of the Green's function is very similar to that found previously. The difference is that we are now computing the Green's function for a periodic, interacting Coupled Cluster Hamiltonian, which subsequently enables the calculation of excited state properties. To further cement this idea, we can demonstrate that the

Lehmann representation of the Green's Function is easily recovered if we introduce a resolution of the identity over all (N-1) and (N+1) eigenstates:

$$G_{pk_pqk_q}(\omega) = \sum_{\mu} \frac{< \Phi|(1+\Lambda)\bar{c}_{pk_p}|\Phi_\mu^{N+1} >< \Phi_\mu^{N+1}|\bar{c}^\dagger_{qk_q}|\Phi >}{\omega - (E_\mu^{N+1} - E_0) + i\eta} \tag{4.7}$$

$$+ \sum_{\nu} \frac{< \Phi|(1+\Lambda)\bar{c}^\dagger_{qk_q}|\Phi_\nu^{N-1} >< \Phi_\nu^{N-1}|c_{pk_p}|\Phi >}{\omega - (E_0 - E_\nu^{N-1}) + i\eta} \tag{4.8}$$

Where we used:

$$Q^{(N+1)}\bar{H}Q^{(N+1)} = \sum_{\mu} |\psi_\mu^{N+1} > E_\mu^{N+1} < \psi_\mu^{N+1}| \tag{4.9}$$

$$Q^{(N-1)}\bar{H}Q^{(N-1)} = \sum_{\nu} |\psi_\nu^{N-1} > E_\nu^{N-1} < \psi_\nu^{N-1}| \tag{4.10}$$

and the Q operators represent the projection operators onto the (N+1) and (N-1) Hilbert spaces. In this familiar form, the ionization potentials and electron affinities appear in the denominator as poles of our Coupled Cluster Green's Function. Now it is apparent why the Coupled Cluster approach is useful: through knowledge of the excitation operator $\hat{T}$, our reference determinants, and other intermediates available from Coupled Cluster, we can directly evaluate the matrix elements of our Green's Function and determine the quasiparticle energies.

Chapter 5

SPECTRAL FUNCTIONS AND ANGLE-RESOLVED PHOTOELECTRON SPECTROSCOPY (ARPES)

With the Single-particle Green's Function, we can compute a term that is directly measurable via experiment. This is known as the spectral function, which is written as:

$$S(\omega) = S^{EA}_{pk_pqk_q}(\omega) + S^{IP}_{pk_pqk_q}(\omega) \tag{5.1}$$

$$\begin{aligned} S^{EA}_{pk_pqk_q}(\omega) &= -\frac{1}{\pi} Im\ G^{EA}_{pk_pqk_q}(\omega) \\ &= \sum_{\mu} < \Phi|(1+\Lambda)\bar{c}_{qk_q}|\Phi^{N+1}_{\mu} >< \Phi^{N+1}_{\mu}|\bar{c}^{\dagger}_{pk_p}|\Phi > \delta(\hbar\omega - (E^{N+1}_{\mu} - E^{N}_{0})) \end{aligned} \tag{5.2}$$

$$\begin{aligned} S^{IP}_{pk_pqk_q}(\omega) &= \frac{1}{\pi} Im\ G^{IP}_{pk_pqk_q}(\omega) \\ &= \sum_{\nu} < \Phi|(1+\Lambda)\bar{c}^{\dagger}_{qk_q}|\Phi^{N-1}_{\nu} >< \Phi^{N-1}_{\nu}|\bar{c}_{pk_p}|\Phi > \delta(\hbar\omega - (E^{N}_{0} - E^{N-1}_{n})) \end{aligned} \tag{5.3}$$

Where we used the relation that for $\eta = 0^+$,

$$Im\frac{1}{x+i\eta} = -\frac{\eta}{x^2+\eta^2} = -\pi\delta(x) \tag{5.4}$$

The signals at the EA and IP energies can be clearly seen in the delta function. The spectral function's intensity is given by the overlap between the (N-1) or (N+1) excited state wavefunctions and the ground state N electron wavefunction. The diagonal part of the spectral function can be interpreted as the probability of the electron removal or electron addition process. We can thus probe the band structure for our given periodic system via computing this term for each point along a Brillouin zone path.

The spectral function is accessible experimentally through Angle-Resolved Photoemission spectroscopy (ARPES) [18]. This technique probes the spectral function via its relationship to the intensity I of the measured signal:

$$I(k, \omega, e_\nu, \nu) = \sum_{n}^{occ} I_0(n, k, \omega, e_\nu, \nu) f(\omega) S_{n,k}(\omega) \tag{5.5}$$

Here e_ν represents the polarization and ν the incident photon frequency. I_0 gives the absorption cross section of the incident photons and f is the Fermi Dirac distribution.

Chapter 6

COMPUTATIONAL APPROACH

We evaluate the Coupled Cluster Green's function by defining intermediate operators in the (N-1) and (N+1) space by which to partition the calculation of matrix elements. In Bhaskaran et al. they are denoted as $X_p(\omega)$ and $Y_q(\omega)$ [9]. For periodic systems, they can then be defined as:

$$(\omega + (\bar{H} - E_0) - i\eta)X_{pk_p}(\omega)|\Phi >= \bar{c}_{pk_p}|\Phi > \tag{6.1}$$

$$(\omega - (\bar{H} - E_0) - i\eta)Y_{qk_q}(\omega)|\Phi >= \bar{c}^{\dagger}_{qk_q}|\Phi > \tag{6.2}$$

Which allows us to rewrite equations (4.7) and (4.8) as:

$$G_{pk_pqk_q}(\omega) =< \Phi|(1+\Lambda)\bar{c}^{\dagger}_{qk_q}X_{pk_p}(\omega)|\Phi > + < \Phi|(1+\Lambda)\bar{c}_{pk_p}Y_{qk_q}(\omega)|\Phi > \tag{6.3}$$

We see now that calculation of the matrix elements can be broken down into two distinct parts - one must compute the coefficients of $X_{pk_p}(\omega)$ and $Y_{qk_q}(\omega)$ and contract them with the remaining left-side determinants, $< \Phi|(1 + \Lambda)\bar{c}^{\dagger}_{qk_q}$ and $< \Phi|(1 + \Lambda)\bar{c}_{pk_p}$. We will now denote these left-side determinants as $e_{q/p}$ for brevity.

Formally, the operators $X_{pk_p}(\omega)$ and $Y_{qk_q}(\omega)$ take the following forms when we consider CCSD:

$$X_{pk_p}(\omega) = \sum_{k_i,i} x_{ik_i}(\omega)_{pk_p}c_{ik_i} + {\sum_{k_i,k_j,ka}}' \sum_{i<j,a} x^{ak_a}_{ik_i,jk_j}(\omega)_{pk_p}c^{\dagger}_{ak_a}c_{jk_j}c_{ik_i} \tag{6.4}$$

$$Y_{qk_q}(\omega) = \sum_{k_a,a} y^{k_a}(\omega)_{qk_q}c^{\dagger}_{ak_a} + {\sum_{k_a,k_b,k_i}}' \sum_{a<b,i} y^{ak_abk_b}_{ik_i}(\omega)_{qk_q}c^{\dagger}_{ak_a}c^{\dagger}_{bk_b}c_{ik_i} \tag{6.5}$$

It is clear that these operators are defined on the (N+1) and (N-1) particle spaces from the string of electron creation and annihilation operators contained within. Note that the primed summations again imply the conservation of crystal momenta. In practice, this allows for summations over three k-point indices to be lowered to sumations over two indices through equation (3.7), leading to reduced scaling with k.

Equations (6.1) and (6.2) can be evaluated diagrammatically through taking advantage of the Campbell-Baker-Hausdorff formula to write the exponentiated creation and annihilation operators as:

$$\bar{c}_p = c_p + [c_p, \hat{T}] \tag{6.6}$$

$$\bar{c}_p^\dagger = c_p^\dagger + [c_p^\dagger, \hat{T}] \tag{6.7}$$

Working equations for the non-periodic form of $\bar{c}_{pk_p}|\Phi>$, $\bar{c}^\dagger_{qk_q}|\Phi>$ and $e_{p/q}$ vectors have been outlined extensively in the publication by Nooijen and Bartlett. Furthermore, the operator contractions $\bar{H}X_{pk_p}(\omega)|\Phi>$ and $\bar{H}Y_{qk_q}(\omega)|\Phi>$, which are necessary to solve equations (6.1) and (6.2), correspond to those found in the traditional EOM-CC methods [19]. We shall not further discuss them here, except to mention that the relevant k-indices per Bloch orbital and momentum conservation must be included and summed over in the periodic case [8].

One special consequence of our analysis is that, for general orbital indices p and q used to express our Green's function, k_p must equal k_q. This is due to momentum conservation with the creation and subsequent annihilation of quasiparticles. Thus, in practice, G_{pq} is calculated for a single k-point index at a time.

In summary, we compute matrix elements of the Coupled Cluster Green's Function per k-point by solving equation (6.3). This involves evaluation of the intermediates $X_{pk_p}(\omega)$ and $Y_{qk_q}(\omega)$ through solving the linear equations (6.1) and (6.2). The result is then contracted with the left-hand determinant e for each general orbital index.

Chapter 7

PRELIMINARY RESULTS

The Periodic Coupled Cluster Singles-Doubles Green's Function method (KCCSD-GF) for restricted spatial orbitals was implemented in PySCF as part of the existing "PBC" framework.

As a proof of concept, a calculation was performed starting from a Hartree-Fock reference to obtain the Green's function for a Diamond lattice with a 2x2x2 Monkhorst-Pack grid along a Brillouin-zone path of 50 points (Fig 7.1, x axis). The GTH norm-conserving pseudopotential [20] was used for the core electrons along with the corresponding single-zeta basis set (gth-SZV). The Green's function was computed on an energy (ω) grid of of 150 evenly spaced points between -1.0 and 1.0 Hartree (Fig 7.1, y axis). The spectral functions were subsequently obtained for each point along the k-path and the intensity (Fig 7.1, z axis) plotted against the energy and k-path to obtain the band structure:

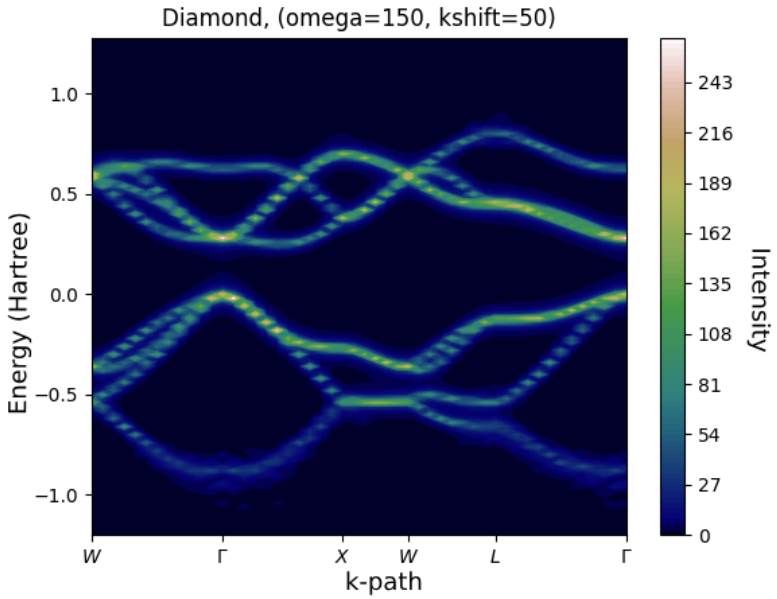

Figure 7.1: Computed band structure for the Diamond lattice using the gth-SZV basis set. The behavio rof the electornic bands at the high symmetry behavior is reproduced at the special points along the x-axis

The computed band gap at Γ was found to be 5.62 eV, which slightly overestimates the reference value of 5.47 eV [21]. This may be due to the large finite-size effects associated with the small k-point grid used in the calculation. We expect to achieve a more accurate description upon extrapolation of the Brillouin-zone sampling to the thermodynamic limit.

The peaks of the spectral function for each point along the Brillouin zone path represent excitations with high single-particle character. In the lowest satellite state between the W and X special points, there is a noticeable smearing in the intensity of the spectral function. This is theorized to be due to stronger many-body interactions, and may be better resolved as we include greater correlation effects in our approximation.

Although we have shown that the KCCSD-GF method can be used to probe the electronic structure of smaller systems, its high cost (N^5) and dependence on ω means that calculations with larger k-point and energy grids quickly become demanding to compute. Because we wish to eliminate error due to finite-size effects, larger calculations are necessary to establish proper extrapolation schemes.

Extrapolation to the basis set limit is also important in the determination of accurate chemical properties. Even CCSD(T), considered the ”gold standard" of computational methods, requires large basis sets for the best results [22]. One method that we have explored towards this end is the truncation of the virtual space associated with larger basis sets to mitigate the sizable cost increase. This has been accomplished in several ways in the past, including the SCF method and the Frozen Natural Orbitals (FNO) method [23, 24].

The former method attempts to eliminate the linear dependencies present in correlated calculations through removal of high energy virtual orbitals in the SCF step. The latter involves obtaining frozen natural orbitals from the virtual-block of the second-order Moller Plesset density matrix and performing the truncation based on the resulting occupation numbers:

$$D^{(2)}_{ab} = \frac{1}{2} \sum_{cij} \frac{< cb||ij >< ij||ca >}{\epsilon^{cb}_{ij} \epsilon^{ca}_{ij}} \tag{7.1}$$

Where D represents the MP2 density matrix and the corresponding eigenvectors and eigenvalues are the natural orbitals and occupancies.

Both methods were implemented into the KCCSD-GF code and compared for various truncations of the virtual space. Although the FNO method has been traditionally

shown to be better than the SCF method for maintaining the ground-state properties [25], it performed noticeably worse when computing spectral functions. The following are those computed for a Diamond lattice sampling a 2x1x1 k-point mesh along Γ for computational ease. The x-axis denotes the energy range on which the function was calculated, and the y-axis denotes the intensity of the function.

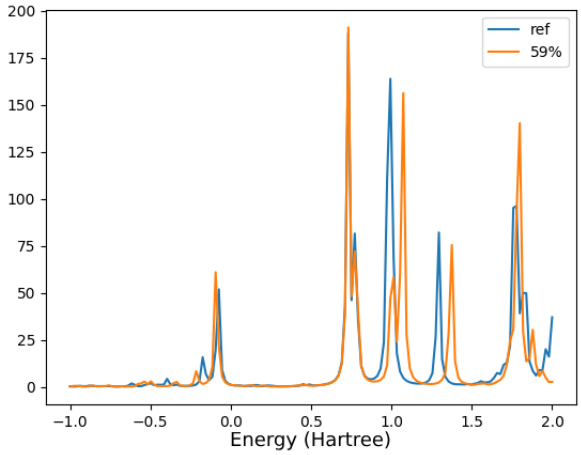

Figure 7.2: The spectral function computed for a Diamond lattice with 59 percent of the virtual space as determined from the FNO method. It performs noticeably worse than that obtained from the SCF method, with differences in not only peak intensity but also relative peak location, corresponding to inaccurate shifts in the energy spectrum.

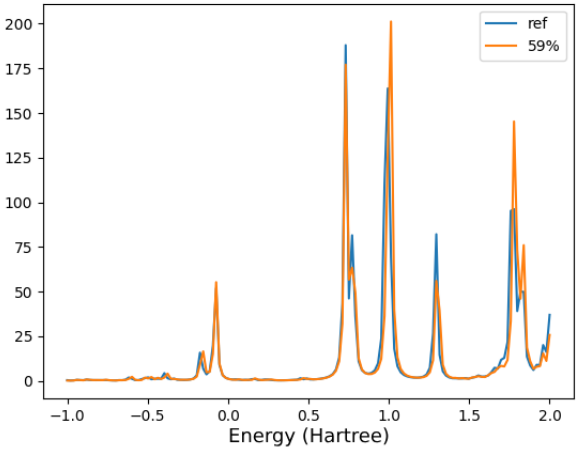

Figure 7.3: The spectral function for a Diamond lattice computed from the SCF method.

Chapter 8

FUTURE DIRECTIONS

The truncation of the virtual space is a good first step towards reducing the cost of computing Coupled Cluster Green's Functions. One area of further effort will most certainly be towards finding the optimal method which best preserves the values of the spectral functions, furthering the basic analysis started above.

In this spirit, it is also prudent to consider the linear solver as an area for further optimization. Currently, the KCCSD-GF implementation uses NumPy's implementation of the Generalized Conjugate Residual method (GCROT) to solve the linear equation for the intermediates $X_{pk_p}(\omega)$ and $Y_{qk_q}(\omega)$ [26]. Using a faster implementation for this step, which is the computational bottleneck for the method, is sure to achieve considerable speed-up.

Once we are able to apply KCCGF for larger k-point grids and basis sets, we intend to study the electronic structure of materials of technological interest. One such material is graphene, which can be layered to control its band gap and resulting electronic properties [27]. ARPES spectra of monolayer graphene is also available, which provides a convenient basis for comparison with the KCCGF method [28]. As a first step, we performed a small band-structure calculation on a graphene sheet with a 3x3 k-grid and SZV basis.

There are a few observations that can be made from this result. First, it is clear that the band resolution is poor not just at the satellites, but at bands close to the Fermi-level as well. Several spurious peaks also occur at the beginning and end of the k-path along with discontinuities in the band structure, possibly due to errors in the initial mean-field calculation. These issues typically originate from systems which possess metallic character, and require large k-point grids in order to properly converge. Our desire to achieve greater accuracy through sampling larger areas of the Brilluoin zone, in conjunction with these technical issues, motivate the optimization of the KCCSD-GF method.

We expect to observe linear dispersion near the Dirac-point for an isolated graphene sheet. Once we are able to scale up the mesh of k-points sampled and achieve efficient representations of the virtual space for larger basis sets, we may begin a more detailed analysis of the Fermi velocity renormalization, plasmon satellites, and more [29].

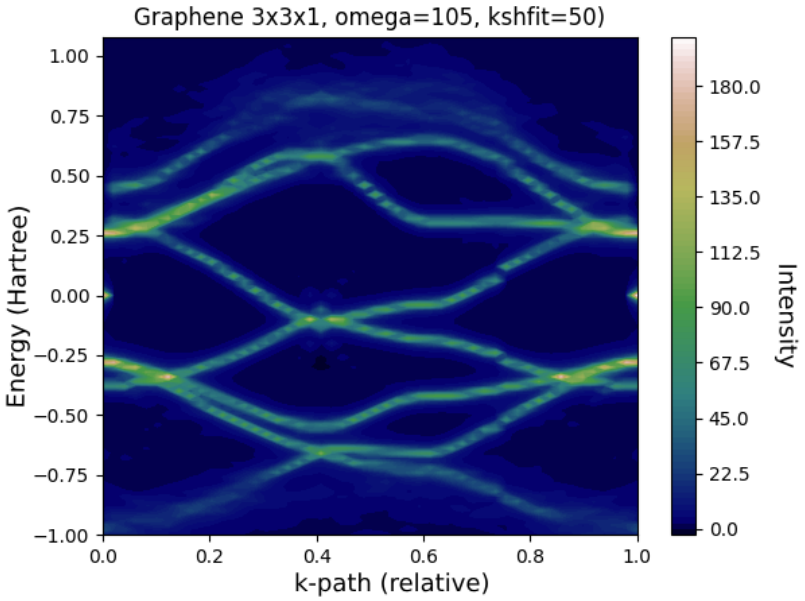

Figure 8.1: Band structure for Graphene sheet with an energy grid consisting of 105 evenly spaced points between -1 and 1 and a k-path consisting of 50 points.

Our goal is to then perform a comparison with analyses previously conducted with the $G.W.$ method [30, 31]. These characteristics have been noticeably harder to find with the EOM-KCCSD method reported in [14], which struggles to converge roots corresponding to satellite states during the Davidson routine.

Chapter 9

CONCLUSIONS

In the above, we have outlined the implmentation of a Restricted Coupled Cluster Singles-Doubles Green's Function method for periodic systems and outlined an initial calculation of the band structure of Diamond for a 2x2x2 k-point sampling and gth-SZV basis set. We intend to optimize the algorithm's primary bottlenecks, such as computation of the intermediates $X_{pk_p}(\omega)$ and $Y_{qk_q}(\omega)$, to enable calculations with larger basis sets and k-point grids in pursuit of accurate extrapolation schemes. Once we reach a point where extrapolation is achievable, we intend to compute accurate electronic spectra for solids of interest to the fields of condensed matter physics and materials science.

BIBLIOGRAPHY

(1) Von Niessen, W.; Schirmer, J.; Cederbaum, L. *Comput. Phys. Rep.* **1984**, *1*, 57–125.

(2) Hedin, L. *Phys. Rev.* **Aug. 1965**, *139*, A796–A823.

(3) Aryasetiawan, F.; Gunnarsson, O. *Rep. Prog. Phys.* **1998**, *61*, 237.

(4) Aulbur, W. G.; Jönsson, L.; Wilkins, J. W. In, Ehrenreich, H., Spaepen, F., Eds.; Solid State Physics, Vol. 54; Academic Press: 2000, pp 1–218.

(5) Reining, L. *Wiley Interdiscip. Rev.: Comput. Mol. Sci.* **2018**, *8*, e1344.

(6) Shishkin, M.; Marsman, M.; Kresse, G. *Phys. Rev. Lett.* **2007**, *99*, 246403.

(7) Nooijen, M.; Snijders, J. G. *Int. J. Quantum Chem.* **1992**, *44*, 55–83.

(8) Nooijen, M.; Snijders, J. G. *Int. J. Quantum Chem.* **1993**, *48*, 15–48.

(9) Bhaskaran-Nair, K.; Kowalski, K.; Shelton, W. A. *J. Chem. Phys.* **2016**, *144*, 144101.

(10) Sun, Q.; Berkelbach, T. C.; Blunt, N. S.; Booth, G. H.; Guo, S.; Li, Z.; Liu, J.; McClain, J. D.; Sayfutyarova, E. R.; Sharma, S., et al. *Wiley Interdiscip. Rev.: Comput. Mol. Sci.* **2018**, *8*, e1340.

(11) Odashima, M. M.; Prado, B. G.; Vernek, E. *Rev. Bras. Ensino Fis.* **2017**, *39*.

(12) Bartlett, R. J.; Musiał, M. *Rev. Mod. Phys.* **2007**, *79*, 291.

(13) Crawford, T. D.; Schaefer III, H. F. *Rev. Comput. Chem.* **2000**, 33–136.

(14) Mcclain, J.; Sun, Q.; Chan, G. K.-L.; Berkelbach, T. C. *J. Chem. Theory Comput.* **2017**, *13*, 1209–1218.

(15) Purvis III, G. D.; Bartlett, R. J. *J. Chem. Phys.* **1982**, *76*, 1910–1918.

(16) Noga, J.; Bartlett, R. J. *J. Chem. Phys* **1987**, *86*, 7041–7050.

(17) Hirata, S.; Podeszwa, R.; Tobita, M.; Bartlett, R. J. *J. Chem. Phys* **2004**, *120*, 2581–2592.

(18) Damascelli, A. *Phys. Scr.* **2004**, *2004*, 61.

(19) Nooijen, M.; Bartlett, R. J. *J. Chem. Phys.* **1995**, *102*, 3629–3647.

(20) Goedecker, S.; Teter, M.; Hutter, J. *Phys. Rev. B* **1996**, *54*, 1703.

(21) Koizumi S The Physics of Group IV Semiconductors., University of Exeter.

(22) Rezac, J.; Hobza, P. *J. Chem. Theory Comput.* **2013**, *9*, 2151–2155.

(23) Taube, A. G.; Bartlett, R. J. *J. Chem. Phys.* **2008**, *128*, 164101.

(24) Landau, A.; Khistyaev, K.; Dolgikh, S.; Krylov, A. I. *J. Chem. Phys.* **2010**, *132*, 014109.

(25) Sosa, C.; Geertsen, J.; Trucks, G. W.; Bartlett, R. J.; Franz, J. A. *Chem. Phys. Lett.* **1989**, *159*, 148–154.

(26) Hicken, J. E.; Zingg, D. W. *SIAM J. Sci. Comput.* **2010**, *32*, 1672–1694.

(27) Ohta, T.; Bostwick, A.; Seyller, T.; Horn, K.; Rotenberg, E. *Science* **2006**, *313*, 951–954.

(28) Zhou, S. Y.; Gweon, G.-H.; Fedorov, A.; First PN, d.; De Heer, W.; Lee, D.-H.; Guinea, F.; Neto, A. C.; Lanzara, A. *Nat. Mater.* **2007**, *6*, 770.

(29) Neto, A. C.; Guinea, F.; Peres, N. M.; Novoselov, K. S.; Geim, A. K. *Rev. Mod. Phys.* **2009**, *81*, 109.

(30) Trevisanutto, P. E.; Giorgetti, C.; Reining, L.; Ladisa, M.; Olevano, V. *Phys. Rev. Lett.* **2008**, *101*, 226405.

(31) Lischner, J.; Vigil-Fowler, D.; Louie, S. G. *Phys. Rev. Lett.* **2013**, *110*, 146801.